

Many-body quasiparticle spectrum of Co-doped ZnO: A GW perspectiveI. Abdolhosseini Sarsari,^{1,2} C. D. Pemmaraju,¹ Hadi Salamati,² and S. Sanvito¹¹*School of Physics and CRANN, Trinity College, Dublin 2, Ireland*²*Department of Physics, Isfahan University of Technology, Isfahan, 84156-83111, Iran*

(Received 4 March 2013; published 20 June 2013)

In transition-metal-doped ZnO the energy position of the dopant $3d$ states relative to the host conduction and valence bands determines the possibility of long-range ferromagnetism. Density functional theory (DFT) can estimate the energy position of the Co- $3d$ states in ZnO:Co but this depends substantially upon the choice of exchange-correlation functional. In this paper we investigate many-body GW corrections built on top of DFT + U and hybrid-DFT ground states to provide a theoretical benchmark for the quasiparticle energies in wurtzite ZnO:Co. Both single shot G_0W_0 as well as partially self-consistent GW_0 , wherein the wave functions are held fixed at the DFT level but the eigenvalues in G are iterated, are considered. The predicted energy position of the minority spin Co- t_2 states is 3.0–3.6 eV above the ZnO conduction band minimum, which is closer to hybrid-DFT-based estimates. Such an electronic structure does not support carrier-mediated long-range ferromagnetism at achievable n -doping conditions.

DOI: [10.1103/PhysRevB.87.245118](https://doi.org/10.1103/PhysRevB.87.245118)

PACS number(s): 75.50.Pp, 71.20.–b, 71.55.–i

I. INTRODUCTION

The quest for oxide dilute magnetic semiconductors (DMS) exhibiting high Curie temperature T_C has been ongoing for nearly a decade, driven by the prospect of realizing future spintronic materials incorporating both semiconducting and ferromagnetic properties.¹ ZnO, already of great technological relevance as a transparent conducting oxide exhibiting a multitude of interesting optical and electrical properties,^{2,3} has been widely studied as a potential DMS material following initial reports of room-temperature ferromagnetism (RTF) in Co doped ZnO (ZnO:Co) thin films.⁴ Stabilizing high- T_C ferromagnetism in ZnO in conjunction with its direct and wide band gap, large exciton binding energies, and large piezoelectric constants would lead to a truly multifunctional DMS.⁵ However, after several years of experimental and theoretical investigations a complete explanation of the ferromagnetism in ZnO:Co remains elusive.⁶ Recent experiments suggest a picture wherein ferromagnetism is absent in uniformly doped ZnO:Co single crystal⁷ but emerges in highly defective polycrystalline samples with extended defects such as grain boundaries playing a role.^{8,9}

Numerous theoretical efforts based on density functional theory (DFT) have also investigated the microscopic origins of magnetic interaction between the Co ions in ZnO:Co.^{10–14} In particular, a variety of methods going beyond the local density and the generalized gradient approximations (respectively LDA and GGA) have been employed to mitigate the severe ZnO band-gap underestimation of the LDA/GGA. Such beyond-LDA methods (indicated here collectively as b -LDA) include DFT + U ,¹³ the nonlocal external potential (NLEP) scheme,¹⁵ the atomic self-interaction correction (ASIC) approach¹² and hybrid DFT.¹¹

The description of the ground-state electronic structure of ZnO:Co in the absence of additional charge doping defects is similar in the different b -LDA approaches: Co²⁺ ions doping the Zn site (Co_{Zn}) in wurtzite ZnO are nominally in a d^7 valence configuration, and the approximately tetrahedral crystal field splits the Co- $3d$ states into a set of lower e and higher t_2 like levels (see Fig. 1). The majority-spin e

and t_2 as well as the minority-spin e states are filled, while the minority spin t_2 (t_2^\downarrow) are empty. This leads to a net magnetic moment of $3\mu_B$ per Co_{Zn}. The energy position of the t_2^\downarrow states relative to the host conduction band is however crucial for the ferromagnetism, since it determines whether or not a carrier-mediated mechanism is effective. In general, electron hopping between transition metal (TM) dopant sites hosting partially occupied d states leads to a stabilization of the ferromagnetic interaction.^{16,17} This mechanism is active even in the presence of Jahn-Teller distortions that lift the TM d states degeneracy,^{14,15,17} provided that the d states are resonant within either the conduction or the valence band continuum of the host semiconductor. In this situation their occupancy can be continuously varied. Accordingly, theoretical works in the literature^{12–14} employing a variety of b -LDA approximations indicate that a partial occupancy of the t_2^\downarrow states under extraneous electron doping is a minimum requirement for long-range FM interactions between Co ions in ZnO:Co. Unfortunately, the different approaches differ substantially in their estimates of the position of the t_2^\downarrow states relative to the conduction band minimum (CBM), leading to different predictions for the feasibility of room temperature ferromagnetism in ZnO:Co.^{12–14,18,19}

A scenario where the Co- t_2^\downarrow states are located at or below the CBM¹³ would be conducive to ferromagnetism in ZnO:Co under modest n -doping conditions and without the need for structural defects, whereas if the t_2^\downarrow states were resonant well inside the conduction band, either larger n doping¹⁴ or additional structural defects that lower the position of the t_2^\downarrow states towards the CBM¹² would be necessary. The assumption underlying these predictions based on DFT is the interpretation of the Kohn-Sham (KS) eigenvalues as approximate addition and removal energies, corresponding to photoemission spectra (PES). While no formal justification exists for such an interpretation, b -LDA approaches are generally designed to improve the agreement with experimental PES of either all or a subset of KS eigenvalues. In the absence of date of a direct observation of the empty Co- t_2^\downarrow states by inverse photoemission, we seek to

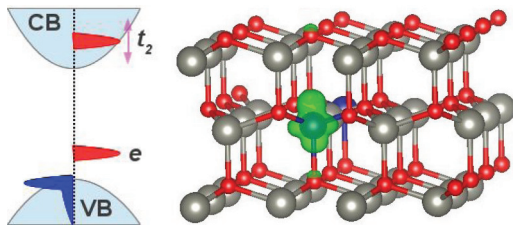


FIG. 1. (Color online) Left: Schematic showing the arrangement of crystal-field split Co-3d states in ZnO:Co relative to host valence bands (VB) and conduction bands (CB). The occupied majority-spin 3d states are shaded deep blue while the minority spin e and t_2 levels are shown in red. Different DFT-based approaches disagree on the placement of the t_2 levels. Right: Periodically repeated supercell of ZnO:Co showing a charge density isosurface for an empty minority-spin Co- t_2 state. The isosurface is plotted for 5% of the maximum value. Large (gray) and small (red) atoms indicate Zn and O, respectively.

resolve the ambiguity in the theoretical description by directly calculating the quasiparticle spectrum of ZnO:Co within the GW approximation.^{20–22}

Many-body perturbation theory based on the GW approximation is a popular approach for calculating the quasiparticle energies of solid-state systems.²³ Many-body effects in the electron-electron interaction that go beyond the mean-field picture are incorporated via the energy-dependent electron self-energy operator Σ , which is approximated as a product of the Green's function G and the dynamically screened Coulomb interaction W . The interaction W is in turn obtained by screening the bare Coulomb interaction with the inverse frequency-dependent dielectric matrix. The GW self-energy corrections are generally calculated on top of the DFT independent-particle KS wave functions and eigenvalues, and the resulting quasiparticle spectra are systematically improved towards direct/inverse photoemission spectra. Different levels of self-consistency are possible within a perturbative GW scheme,²⁴ and in this paper we consider single-shot G_0W_0 as well as partially self-consistent GW_0 , wherein one iterates the eigenvalues in G while keeping W and the wave functions fixed at their DFT estimates. We find that irrespective of the specific b -LDA starting point, the quasiparticle energies of the Co- t_2^\downarrow states are located well above the ZnO CBM. Thus within this picture, partial occupancy of these states is difficult to achieve at any electron doping concentration.

II. METHODS

All the calculations presented in this paper are carried out within the plane-wave-based DFT framework as implemented in the VASP^{25,26} package. A plane-wave kinetic energy cutoff of 300 eV and projector-augmented-wave pseudopotentials²⁷ with the following valence-electron configurations are employed: $3d^{10}4s^2$ for Zn, $2s^22p^4$ for O, and $3d^84s^1$ for Co. The pseudopotentials as well as the starting DFT calculations in this paper employ the Perdew-Burke-Ernzerhof (PBE)²⁸ exchange-correlation functional. Two different b -LDA approaches, namely PBE + U ²⁹ and hybrid DFT,^{30,31} are considered to provide starting points for subsequent GW calculations. The PBE + U calculations use the Hubbard parameters of

$U_{Zn} = 7$ eV, $U_{Co} = 3$ eV, and $J_{Co} = 1$ eV, for the 3d states of Zn and Co, respectively.¹⁴ The larger U for Zn is attributed to a deeper and more localized semicore d^{10} shell in Zn compared to Co. Hybrid-DFT calculations are at the HSE03³¹ level.

For calculations of the ZnO wurtzite unit cell, the Brillouin zone is sampled using a $8 \times 8 \times 6$ Γ -centered k -point mesh. ZnO:Co is modeled with a 32 atom ZnO orthorhombic wurtzite supercell, in which one Zn site is substituted by Co. This corresponds to a nominal Co doping concentration of 6.25%. In the supercell calculations the Brillouin zone is sampled at 28 irreducible k points in a Γ centered mesh. The atomic structures are optimized using the HSE03 functional until the residual forces are smaller than 0.01 eV/Å (0.05 eV/Å) in the primitive cell (supercell). This leads to the following unit-cell parameters for wurtzite ZnO: $a = 3.248$ Å, $c/a = 1.61$, $u = 0.380$. For the GW calculations an energy cutoff of 150 eV is used for the response functions. A total of 240 and 1152 bands are employed in the primitive (wurtzite) cell and supercell calculations, respectively. Both single shot G_0W_0 as well as partially self-consistent GW_0 calculations are carried out on top of DFT-based ground-state starting points. In the GW_0 calculations, the eigenvalues in G are self-consistently updated four times while the orbitals are held fixed as obtained from DFT. Convergence of relevant quasiparticle energies with respect to the number of bands and the response function energy cutoff was studied separately. Details are presented in the Appendix. For the chosen set of simulation parameters a conservative estimate gives us the quasiparticle energies to be converged to within 0.2 eV.

III. RESULTS AND DISCUSSION

A. ZnO unit cell

In order to set the framework for the ZnO:Co supercell calculations, we first investigate the eigenvalue spectrum of pure ZnO obtained both from DFT as well as from GW . In ZnO the predominant character of the valence band maximum (VBM) and the CBM is O- $2p$ and Zn- $4s$, respectively. The Zn- $3d$ states are fully occupied and are located several eV below the VBM. The computed band gaps and Zn- $3d$ binding energies are reported in Table I. ZnO is a prototypical case

TABLE I. Calculated band gap ΔE and average binding energy of Zn- $3d$ states E_{3d} in pure ZnO from different levels of theory are compared to experiments (Refs. 32 and 33). All energies are given in eV.

Method	ΔE (eV)	E_{3d} (eV)
PBE	0.78	5.15
PBE + G_0W_0	2.27	6.05
PBE + GW_0	2.68	6.39
PBE + U	1.58	6.98
PBE + U + G_0W_0	2.62	6.69
PBE + U + GW_0	2.85	6.63
HSE	2.24	6.01
HSE + G_0W_0	3.14	6.64
HSE + GW_0	3.31	6.81
Expt.	3.44	7.5–8.81

for extreme band gap ΔE , underestimation by local/semilocal exchange-correlation functionals. The predicted ΔE from the PBE functional for instance is 0.78 eV, while the experimental one is 3.44 eV.³² Some part of this band-gap underestimation can be traced to the too low binding energy of the cation $3d$ states and their concomitant hybridization with the anion $2p$ states in the valence band. The average Zn- $3d$ binding energy E_{3d} from PBE is ~ 5.1 eV compared to 7.5–8.81 eV in experiments.³³ Given a bandwidth of ~ 5.5 eV for the O- $2p$ valence band, this leads to spurious Zn- $3d$ /O- $2p$ hybridization, which because of p - d repulsion pushes the O- $2p$ states higher in energy reducing ΔE . This effect, which can be traced to the self-interaction error, is over and above the conventional DFT underestimation of band gaps in semiconductors.³⁴

A significant improvement in the value of ΔE can be obtained simply by correcting for the low binding energy of the Zn- $3d$ states. Accordingly, the inclusion of a Hubbard- U correction on the Zn- $3d$ states within PBE + U results in $E_{3d} \sim 7$ eV, while also improving ΔE to 1.58 eV. This nevertheless still represents an almost 50% underestimation of ΔE . The description can be further improved by employing a hybrid-DFT functional such as HSE03. The inclusion of nonlocal Fock exchange not only leads to a reduction in the self-interaction error, but to a large extent also restores the derivative discontinuity in the exchange-correlation functional within a generalized Kohn-Sham (GKS) scheme,³⁰ further improving the band gap. Thus HSE03 predicts values of ΔE and E_{3d} at 2.24 eV and 6 eV, respectively.

Perturbative G_0W_0 corrections on top of the DFT starting wave functions lead to systematic improvements in the resulting quasiparticle spectrum. We see from Table I that, irrespective of the starting DFT XC functional, both ΔE and E_{3d} calculated with G_0W_0 are corrected towards the experimental values, and including partial self-consistency through GW_0 further improves the agreement. Nevertheless, the actual value of ΔE is seen to depend upon the DFT starting point.³⁴ The use of G_0W_0 on top of PBE (PBE + U) leads to a value of ΔE that is still underestimated by $\sim 34\%$ ($\sim 24\%$). In contrast, the value of ΔE from HSE + G_0W_0 at 3.14 eV is within $\sim 9\%$ of experiments. At the GW_0 level, ΔE is further increased relative to G_0W_0 and is within 22% of experiment irrespective of starting DFT functional. In particular, ΔE from HSE + GW_0 at 3.31 eV matches well with experiments. Similarly, the G_0W_0 and GW_0 quasiparticle shifts generally tend to increase E_{3d} relative to the corresponding DFT starting point and towards the PES value. However, the PBE + U starting point, which includes a large on-site $U_{Zn} = 7$ eV to begin with, seems to be an exception. Quasiparticle corrections in this case are seen to slightly reduce E_{3d} from 6.98 eV in the DFT ground state to 6.63 eV in PBE + U + GW_0 . Overall, the GW approximation leads to an underestimation of about 1–1.5 eV of the $3d$ band irrespective of the starting point as has been noted previously in the literature.³⁴ Our results for ΔE and E_{3d} in Table I are in good agreement with earlier benchmark calculations on zinc-blende ZnO^{24,34} taking into account that ΔE in wurtzite ZnO is expected to be ~ 0.2 eV larger.³⁴

B. ZnO:Co supercell

Co substituting Zn (Co_{Zn}) in ZnO is formally in a Co^{2+} oxidation state with seven electrons in the occupied Co_{3d}

orbitals. The nearly tetrahedral crystal field around Co_{Zn} splits the Co_{3d} states into a set of lower e and higher t_2 orbitals. Furthermore, Co_{Zn} assumes a high-spin configuration with $(e^\uparrow)^2 (t_2^\uparrow)^3$ majority spin and $(e^\downarrow)^2 (t_2^\downarrow)^0$ minority spin occupancies resulting in a local magnetic moment of $3 \mu_B$ per site.

First we briefly discuss the electronic structure of ZnO:Co obtained from ground-state DFT calculations. The LDA/GGA exchange and correlation functionals yield a qualitatively incorrect ZnO:Co ground state^{12,15} by erroneously placing the occupied e^\downarrow levels in resonance with the CBM of ZnO. This results in spurious charge transfer to the host and fractional occupation of the e^\downarrow orbitals. Such an error is due to a combination of underestimating both the host band gap and the binding energy of the Co- $3d$ states. Importantly b -LDA approaches that either partially or fully rectify these shortcomings reproduce the correct occupancy of the e^\downarrow states^{11–13,15} and return a magnetic moment of $3 \mu_B$ per Co_{Zn} . As a general feature, common to the different b -LDA methods, the fully occupied majority spin Co- $3d$ states hybridize with the ZnO O- $2p$ valence band and some Co- $3d$ DOS appears at the top of the host VBM. Different approaches however differ substantially at a quantitative level in their description of the minority spin Co- $3d$ states.

Considering the case of PBE + U with $U_{Zn} = 7$ eV and $U_{Co} = 3$ eV, $J_{Co} = 1$ eV, we find that even though ΔE is still underestimated, the e^\downarrow orbitals are correctly occupied by two electrons and are located approximately 1.2 eV above the host VBM (see Fig. 2 and Table II). Meanwhile, the empty t_2^\downarrow states are resonant in the conduction band with an onset at roughly 1.6 eV above the CBM and 3.3 eV above the host

TABLE II. Summary table of the electronic structure of Co-doped ZnO. Here E_{e^\downarrow} , $E_{t_2^\downarrow}$, indicating the energy positions of the Co e^\downarrow and t_2^\downarrow states relative to the host valence band top are presented for different levels of theory. Results from supercell calculations both with and without an oxygen vacancy (V_O) next to the Co are presented. $E_{t_2^\downarrow} - \Delta E$ indicates the position of the t_2^\downarrow states relative to the CBM. The last column gives the position of the t_2^\downarrow states relative to the CBM if the latter is shifted rigidly to reproduce the experimental band gap (ΔE^{exp}) while holding $E_{t_2^\downarrow}$ fixed.

Name	E_{e^\downarrow}	$E_{t_2^\downarrow}$	$E_{t_2^\downarrow} - \Delta E$	$E_{t_2^\downarrow} - \Delta E^{\text{exp}}$
ZnO:Co				
PBE + U	1.2	3.3	1.6	−0.1
PBE + U + G_0W_0	1.3	5.3	2.5	1.9
PBE + U + GW_0	1.4	6.1	3.0	2.6
HSE	0.6	5.0	2.7	1.6
HSE + G_0W_0	0.7	6.6	3.3	3.2
HSE + GW_0	0.8	7.1	3.6	3.7
ZnO:Co + V_O				
PBE + U	0.5	2.1	0.4	−1.4
PBE + U + G_0W_0	0.8	3.5	0.9	0.0
PBE + U + GW_0	0.9	4.1	1.3	0.7
HSE	0.0	3.6	1.3	0.1
HSE + G_0W_0	0.1	4.6	1.3	1.2
HSE + GW_0	0.2	5.1	1.6	1.6

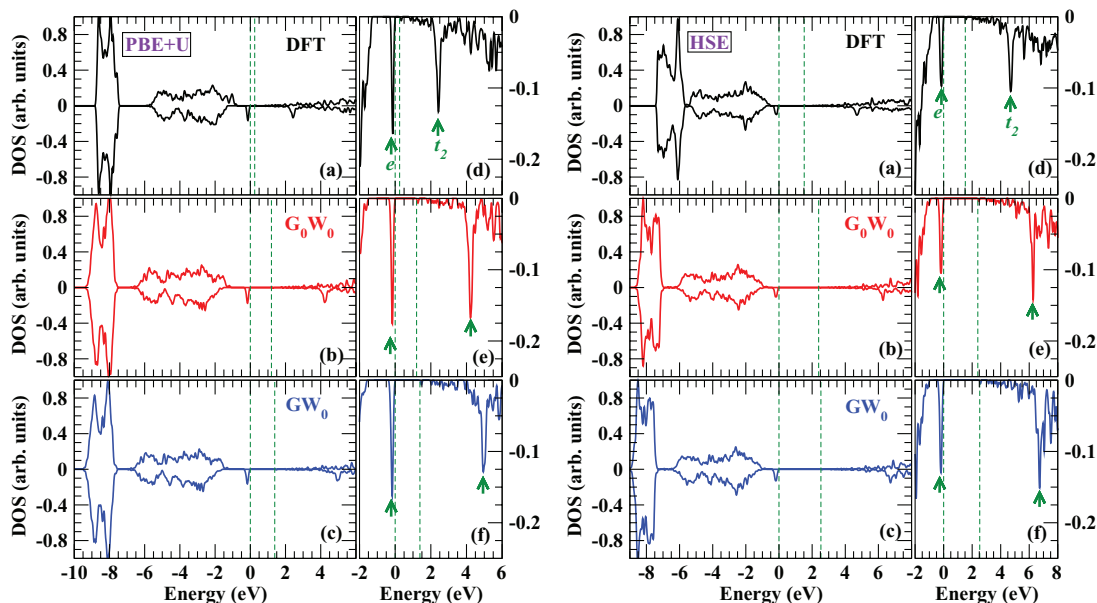


FIG. 2. (Color online) Calculated ZnO:Co density of states (DOS) for a Co dopant concentration of 6.25%. The DOS from two ground-state DFT starting points, namely PBE + U (left), HSE (right), and the corresponding G_0W_0 and GW_0 corrections on top of either are shown. Panels (d)–(f) in either case show a zoomed-in view of the minority-spin DOS around the Fermi energy. Green arrows indicate the positions of the Co-derived minority-spin e and t_2 states. Lower and higher dashed lines indicate the positions of the Fermi energy and of the conduction band minimum, respectively. The Fermi energy in each case is aligned to 0 eV.

VBM. Note, however, that the CBM is still too low in energy as $\Delta E \approx 1.6$ eV. Within PBE + U and related approaches, the positions of the minority spin e^\downarrow , t_2^\downarrow states with respect to the host VBM (these are respectively denoted by E_{e^\downarrow} , $E_{t_2^\downarrow}$) are largely determined by the choice of the parameter U_{Co} . These quantities E_{e^\downarrow} , $E_{t_2^\downarrow}$ are insensitive to additional on-site corrections employed on the Zn-4s orbitals, within a DFT + U approach to also rectify the host CBM position. Therefore if ΔE is restored to its full value of 3.44 eV within such a description,¹³ the empty t_2^\downarrow states would be approximately resonant with the host CBM suggesting that they could be partially occupied at relatively small electron doping concentrations.

The picture that emerges from the HSE functional, while qualitatively similar to that of PBE + U , is quantitatively rather different. We find that E_{e^\downarrow} at ~ 0.6 eV is slightly smaller than in PBE + U but $E_{t_2^\downarrow}$ is substantially larger at ~ 5.0 eV. The inclusion of a fraction of Fock-exchange generally pushes up unoccupied states higher in energy and so the increased value of $E_{t_2^\downarrow}$ is expected. A similar result was found with other hybrid functionals in the past.¹¹ With $\Delta E \sim 2.3$ eV, the onset of the t_2^\downarrow states is roughly 2.7 eV above the host CBM, which renders partial occupancy of these states impossible for any reasonable electron doping level. Even assuming the full experimental value for ΔE , by rigidly shifting the Zn-4s CBM higher in energy while keeping the Co-3d states fixed, leaves the t_2 states about 1.6 eV above the CBM. Thus, starkly different implications emerge from PBE + U and HSE for carrier mediated ferromagnetism in ZnO:Co. A natural question then arises as to which of these two b -LDA descriptions is closer to the actual quasiparticle picture.

In Fig. 2 we also present the DOS for ZnO:Co calculated from G_0W_0 and GW_0 applied on top of PBE + U and HSE. In general, the final quasiparticle spectrum both at the G_0W_0 and GW_0 levels depends to some extent on the DFT starting point. In particular, note that perturbative G_0W_0 and GW_0 corrections applied on top of the qualitatively incorrect PBE ZnO:Co ground state (not shown) do not lead to any improvement and are therefore of little interest. In contrast, b -LDA ground-state starting points lead to more systematic results. We see that the quasiparticle shift of E_{e^\downarrow} is rather small irrespective of the underlying DFT functional. Accordingly E_{e^\downarrow} occurs at 1.3 eV (1.4 eV) for G_0W_0 (GW_0) on top of PBE + U and at 0.7 eV (0.8 eV) for G_0W_0 (GW_0) on top of HSE. An opposite behavior is found for $E_{t_2^\downarrow}$, which not only shows a larger quasiparticle shift but the shift is also invariably towards higher energies compared to the b -LDA starting point. On top of PBE + U , G_0W_0 (GW_0) leads to $E_{t_2^\downarrow}$ of 5.3 eV (6.1 eV), which places the onset of the empty t_2^\downarrow states ~ 2.5 eV (3.0 eV) above the calculated host CBM. Thus the t_2^\downarrow quasiparticle levels are predicted to be much higher in the conduction band than suggested by PBE + U at the DFT level. Even assuming the full value of ΔE , as above, puts the t_2^\downarrow states about 1.9 eV (2.6 eV) higher than the CBM in G_0W_0 (GW_0).

Similarly, G_0W_0 (GW_0) on top of HSE yields a $E_{t_2^\downarrow}$ of 6.6 eV (7.1 eV) with the onset of the t_2^\downarrow states 3.3 eV (3.6 eV) above the corresponding calculated CBM. Based on these results for different DFT starting points, we estimate the onset of the t_2^\downarrow states to be 3.0–3.6 eV above the CBM of ZnO. We find that the magnitude of the quasiparticle shifts relative to the DFT starting point are smaller for HSE than PBE + U . The overall change in $E_{t_2^\downarrow}$ going from the DFT starting point to GW_0 is

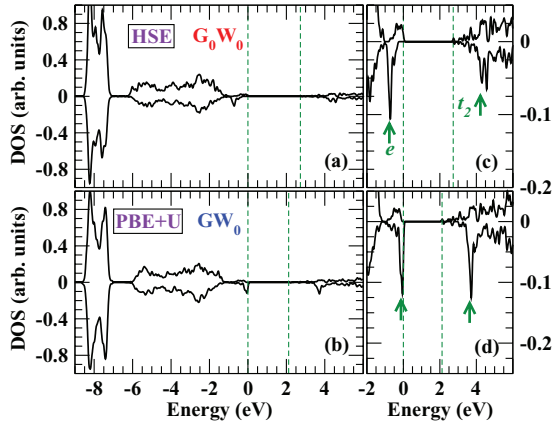


FIG. 3. (Color online) Calculated density of states (DOS) for a ZnO:Co supercell containing a Co_{Zn} and oxygen vacancy (V_{O}) pair. The DOS obtained from G_0W_0 on top of HSE and from GW_0 on top of PBE + U are shown. Panels (c)–(d) show a magnified view of the DOS around the Fermi energy. Green arrows indicate the positions of the Co derived minority-spin e and t_2 states. Lower and higher dashed lines indicate the positions of the Fermi energy and of the conduction band minimum respectively. The Fermi energy is aligned to 0 eV.

2.1 eV and 2.8 eV in HSE and PBE + U , respectively, while the change in $E_{t_2^\downarrow}$ with respect to the CBM (see $E_{t_2^\downarrow} - \Delta E$ in Table II) also shows a similar trend, respectively, at 0.9 eV and 1.4 eV in HSE and PBE + U . A comprehensive study by Fuchs *et al.*³⁴ gave evidence that for a wide range of materials, the overall best agreement with the experimental spectra is obtained at the HSE + G_0W_0 level. At this level, the Co t_2^\downarrow onset is predicted to be 3.3 eV above the CBM, which we offer as the best compromise estimate. This precludes the possibility of FM interactions being mediated by partial occupancy of t_2^\downarrow states under electron doping in the absence of additional structural defects.

Next we investigate the effect of low oxygen co-ordination around Co_{Zn} on the e^\downarrow and t_2^\downarrow quasiparticle energies. In an earlier work¹² on ZnO:Co based on a self-interaction corrected approach,^{35,36} we proposed that oxygen vacancies (V_{O}) next to Co_{Zn} could lower the energy of the t_2^\downarrow states enough to make partial occupancy of these states feasible at reasonable electron doping levels. In this context, we consider one Co_{Zn} + V_{O} pair in a nearest neighbor configuration within a 32 atom supercell of ZnO and calculate the quasiparticle energy levels for this system at the G_0W_0 and GW_0 level based on both PBE + U and HSE starting points. The oxygen vacancy is created by removing one out of the three O atoms co-ordinating the Co_{Zn} in the ZnO wurtzite ab plane. The calculated DOS for this system for representative cases is presented in Fig. 3, and relevant energy levels are reported in Table II.

We find that the effect of V_{O} next to Co_{Zn} is that of lowering both E_{e^\downarrow} and $E_{t_2^\downarrow}$. In fact the energy of all the occupied Co- $3d$ manifold is lowered because of the smaller ligand field acting on Co_{Zn} .¹² Relative to the case of an isolated Co_{Zn} , E_{e^\downarrow} for the Co_{Zn} + V_{O} pair is lower by 0.7 eV in PBE + U and by 0.5 eV (0.6 eV) within G_0W_0 (GW_0) applied on top of the PBE + U electronic structure. The effect on $E_{t_2^\downarrow}$ is even larger as the crystal-field induced splitting between the e^\downarrow and the

t_2^\downarrow orbitals is also reduced. Thus at the PBE + U + G_0W_0 level $E_{t_2^\downarrow}$ for a Co_{Zn} + V_{O} pair is lower by almost 2 eV relative to the case of an isolated Co_{Zn} . The trends observed for G_0W_0 and GW_0 on top of the HSE ground state are similar. The reduction in E_{e^\downarrow} in this case places the e^\downarrow states almost at the VBM while $E_{t_2^\downarrow}$ is seen to decrease by about 2.0 eV.

However, the final alignment of the t_2^\downarrow states relative to the CBM in the GW picture is still not favorable for driving carrier mediated FM. Depending on the level of approximation, the onset of the t_2^\downarrow states is between 0.9 eV and 1.6 eV above the CBM with HSE + G_0W_0 yielding a value of 1.3 eV. This sets a very high electron-doping threshold¹⁵ to achieve partial occupancy even for Co_{Zn} + V_{O} pairs. Thus, at the level of the GW approximation considered in this work, the perspective that emerges is decidedly more pessimistic for carrier mediated FM interactions between Co_{Zn} in ZnO:Co. We note that test calculations including self-consistency in the eigenvalues in both G and W also produce qualitatively similar results with the quasiparticle shifts being slightly larger in the same direction. In this work, we did not consider self-consistency in the quasiparticle wave functions³⁷ taking the off-diagonal terms in the GW Hamiltonian also into account but we do not expect the corrections from such an approach to change the nature of the outcome.

We should point out that our results do not rule out alternative mechanisms for short range ferromagnetic interactions between Co_{Zn} mediated by defects such as H interstitials in specific bonding geometries,³⁸ or some amount of t_2^\downarrow occupancy via s - d hybridization in the case of Co_{Zn} directly bonded to shallow-donor defects such as Zn interstitials.¹² However, such mechanisms for ferromagnetism are limited either by necessitating peculiar arrangements of Co ions throughout the crystal or by achievable defect concentrations. Finally we comment on the observation in recent optical experiments,^{39,40} of excitations to Co- t_2^\downarrow levels at sub-band-gap energies both from the host VBM as well the e^\downarrow states. In order for the GW picture to be consistent with experiment, with the t_2^\downarrow quasiparticle states located well above the host CBM, optical excitations to these levels should be associated with large exciton binding energies of roughly the same amount as $E_{t_2^\downarrow} - \Delta E$. Indeed, while the highly localized nature of the t_2^\downarrow states (see Fig. 1) is compatible with a strong electron-hole interaction energy, a first-principles estimate of the same via the Bethe-Salpeter formalism applied on top of GW ⁴¹ is necessary to reconcile theory and optical experiments.

IV. CONCLUSION

In conclusion, we have investigated the quasiparticle spectrum of Co-doped wurtzite ZnO within a GW framework and with a focus on the minority-spin e^\downarrow and t_2^\downarrow energy levels derived from Co substituting Zn. Single shot G_0W_0 and partially self-consistent GW_0 quasiparticle corrections have been applied on top of two different ground-state DFT starting points based on the PBE + U and HSE exchange-correlation functionals. In general we find the magnitude of the quasiparticle shifts to be smaller in the case of HSE compared to PBE + U . Irrespective of the DFT starting point and the level

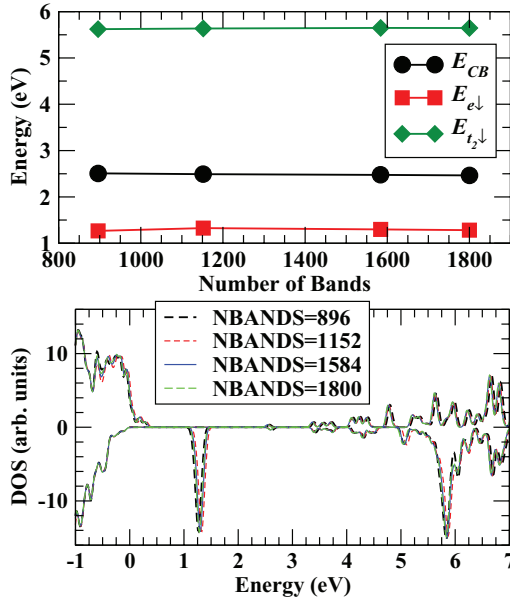


FIG. 4. (Color online) Convergence of calculated quasiparticle energies as a function of the total number of bands (NBANDS). The top panel shows the values of E_{CB} , $E_{e\downarrow}$ and $E_{t_2\downarrow}$ as a function of NBANDS. The bottom panel shows the DOS calculated at different values of NBANDS overlaid.

of GW self-consistency, quasiparticle corrections are seen to shift the empty $\text{Co}_{\text{Zn}} t_2^\downarrow$ states higher in energy placing them roughly 3.3 eV above the conduction band minimum of ZnO. Low oxygen co-ordination around the Co_{Zn} site lowers the quasiparticle energy position of the t_2^\downarrow states to around 1.3 eV above the conduction band minimum. Our results therefore suggest that partial occupancy of the t_2^\downarrow states by electron doping the host material is difficult to achieve, making a conventional carrier-mediated mechanism for ferromagnetism in ZnO:Co less likely.

ACKNOWLEDGMENTS

This work is funded by the Science Foundation of Ireland (07/IN.1/I945), by the EU-FP7 (iFOX project), and by Isfahan University of technology. Computational resources have been provided by the Trinity Center for High Performance Computing.

APPENDIX: CONVERGENCE OF RESULTS

In the following, we discuss the convergence of calculated G_0W_0 quasiparticle energies with respect to various simulation parameters. Convergence of the calculated quasiparticle energies as a function of the total number of bands (NBANDS) in the calculation is shown in Fig. 4 for the case of G_0W_0 constructed on top of PBE + U . For the purposes of these tests, cutoff energies of 300 eV for the plane-wave basis and 100 eV for the response-function basis are employed. We follow the energy positions of the conduction band (E_{CB}), the minority spin e ($E_{e\downarrow}$), and the onset of the t_2 ($E_{t_2\downarrow}$) states relative to the minority spin valence band maximum. We find that at NBANDS = 1152, which is the value used in obtaining our

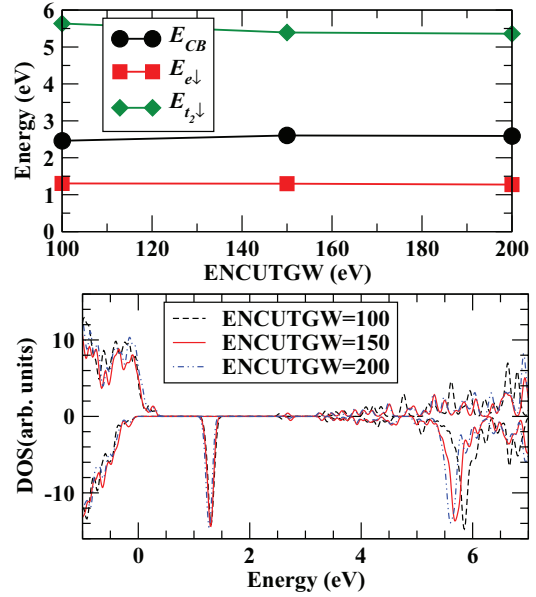


FIG. 5. (Color online) Convergence of calculated quasiparticle energies as a function of the energy cutoff for response functions (ENCUTGW). The top panel shows the values of E_{CB} , $E_{e\downarrow}$, and $E_{t_2\downarrow}$ as a function of ENCUTGW. The bottom panel shows the DOS calculated at different values of ENCUTGW overlaid.

reported results, E_{CB} , $E_{e\downarrow}$, and $E_{t_2\downarrow}$ are respectively converged to within 0.028 eV, 0.043 eV, and 0.009 eV of their values at NBANDS = 1800. Furthermore, the values of these quantities at all four values of NBANDS considered are within 0.059 eV of each other.

Convergence of the calculated quasiparticle energies as a function of the energy cutoff for response functions (ENCUTGW) is shown in Fig. 5 for the case of G_0W_0 on top of PBE + U . For the purposes of these tests a cutoff energy

of 300 eV for the plane-wave basis and a total of 1152 bands (NBANDS = 1152) were employed. For different values of ENCUTGW, we follow the energy positions of the conduction band (E_{CB}), the minority spin e ($E_{e\downarrow}$), and the onset of the t_2 ($E_{t_2\downarrow}$) states relative to the minority spin valence band maximum. We find that at ENCUTGW = 150 eV, which is the value employed in obtaining our reported results, E_{CB} , $E_{e\downarrow}$, and $E_{t_2\downarrow}$ are respectively converged to within 0.012 eV, 0.024 eV, and 0.033 eV of their values at ENCUTGW = 200 eV.

In choosing the k -point grid for the supercell calculations, the following procedure was employed. Initially we benchmarked our GW calculations for the primitive cell of wurtzite ZnO against reference results published using the VASP code.^{24,34} In this case, an $8 \times 8 \times 6$ Γ -centered k -point grid was sufficient to yield good agreement with the reference calculations. For the supercell, we reduced the number of k points along each crystal axis proportionally to the cell dimension along that axis so that the k points were effectively sampled at the same density as in the unit cell calculations. Accordingly, we employed a $2 \times 4 \times 6$ k -point grid in the case of the 32 atom orthorhombic supercell of Co doped ZnO with cell dimensions of $11.32 \text{ \AA} \times 6.54 \text{ \AA} \times 5.24 \text{ \AA}$.

- ¹T. Dietl, H. Ohno, F. Matsukura, J. Cibert, and D. Ferrand, *Science* **287**, 1019 (2000).
- ²Ü. Özgür, Y. Alivov, C. Liu, A. Teke, M. Reshchikov, S. Doğan, V. Avrutin, S. Cho, and H. Morkoc, *J. Appl. Phys.* **98**, 041301 (2005).
- ³Ü. Özgür, D. Hofstetter, and H. Morkoç, *Proc. IEEE* **98**, 1255 (2010).
- ⁴K. Ueda, H. Tabata, and T. Kawai, *Appl. Phys. Lett.* **79**, 988 (2001).
- ⁵A. Janotti and C. G. V. de Walle, *Rep. Prog. Phys.* **72**, 126501 (2009).
- ⁶T. Dietl, *Nat. Mater.* **9**, 965 (2010).
- ⁷T. C. Kaspar, T. Droubay, S. M. Heald, P. Nachimuthu, C. M. Wang, V. Shutthanandan, C. A. Johnson, D. R. Gamelin, and S. A. Chambers, *New J. Phys.* **10**, 055010 (2008).
- ⁸H. S. Hsu, J. C. A. Huang, S. F. Chen, and C. P. Liu, *Appl. Phys. Lett.* **90**, 102506 (2007).
- ⁹B. B. Straumal, A. A. Mazilkin, S. G. Protasova, A. A. Myatiev, P. B. Straumal, G. Schütz, P. A. van Aken, E. Goering, and B. Baretzky, *Phys. Rev. B* **79**, 205206 (2009).
- ¹⁰N. A. Spaldin, *Phys. Rev. B* **69**, 125201 (2004).
- ¹¹C. H. Patterson, *Phys. Rev. B* **74**, 144432 (2006).
- ¹²C. D. Pemmaraju, R. Hanafin, T. Archer, H. B. Braun, and S. Sanvito, *Phys. Rev. B* **78**, 054428 (2008).
- ¹³A. Walsh, J. L. F. Da Silva, and S.-H. Wei, *Phys. Rev. Lett.* **100**, 256401 (2008).
- ¹⁴H. Raebiger, S. Lany, and A. Zunger, *Phys. Rev. B* **79**, 165202 (2009).
- ¹⁵S. Lany, H. Raebiger, and A. Zunger, *Phys. Rev. B* **77**, 241201 (2008).
- ¹⁶P. Mahadevan, A. Zunger, and D. D. Sarma, *Phys. Rev. Lett.* **93**, 177201 (2004).
- ¹⁷H. Raebiger, S. Lany, and A. Zunger, *Phys. Rev. Lett.* **101**, 027203 (2008).
- ¹⁸S. Sanvito and C. D. Pemmaraju, *Phys. Rev. Lett.* **102**, 159701 (2009).
- ¹⁹A. Walsh, J. L. F. Da Silva, and S.-H. Wei, *Phys. Rev. Lett.* **102**, 159702 (2009).
- ²⁰L. Hedin, *Phys. Rev. A* **39**, 796 (1965).
- ²¹M. S. Hybertsen and S. G. Louie, *Phys. Rev. B* **34**, 5390 (1986).
- ²²M. Shishkin and G. Kresse, *Phys. Rev. B* **74**, 035101 (2006).
- ²³F. Aryasetiawan and O. Gunnarsson, *Rep. Prog. Phys.* **61**, 237 (1998).
- ²⁴M. Shishkin and G. Kresse, *Phys. Rev. B* **75**, 235102 (2007).
- ²⁵G. Kresse and J. Furthmüller, *Phys. Rev. B* **54**, 11169 (1996).
- ²⁶G. Kresse and D. Joubert, *Phys. Rev. B* **59**, 1758 (1999).
- ²⁷P. E. Blöchl, *Phys. Rev. B* **50**, 17953 (1994).
- ²⁸J. P. Perdew, K. Burke, and M. Ernzerhof, *Phys. Rev. Lett.* **77**, 3865 (1996).
- ²⁹S. L. Dudarev, G. A. Botton, S. Y. Savrasov, C. J. Humphreys, and A. P. Sutton, *Phys. Rev. B* **57**, 1505 (1998).
- ³⁰A. Seidl, A. Görling, P. Vogl, J. A. Majewski, and M. Levy, *Phys. Rev. B* **53**, 3764 (1996).
- ³¹J. Heyd, G. E. Scuseria, and M. Ernzerhof, *J. Chem. Phys.* **118**, 8207 (2003).
- ³²C. Kittel, *Introduction to Solid State Physics* (Wiley, New York, 1986).
- ³³L. Ley, R. A. Pollak, F. R. McFeely, S. P. Kowalczyk, and D. A. Shirley, *Phys. Rev. B* **9**, 600 (1974).
- ³⁴F. Fuchs, J. Furthmüller, F. Bechstedt, M. Shishkin, and G. Kresse, *Phys. Rev. B* **76**, 115109 (2007).
- ³⁵C. D. Pemmaraju, T. Archer, D. Sánchez-Portal, and S. Sanvito, *Phys. Rev. B* **75**, 045101 (2007).
- ³⁶A. Filippetti, C. D. Pemmaraju, S. Sanvito, P. Delugas, D. Puggioni, and V. Fiorentini, *Phys. Rev. B* **84**, 195127 (2011).
- ³⁷M. Shishkin, M. Marsman, and G. Kresse, *Phys. Rev. Lett.* **99**, 246403 (2007).
- ³⁸C. H. Park and D. J. Chadi, *Phys. Rev. Lett.* **94**, 127204 (2005).
- ³⁹K. R. Kittilstved, W. K. Liu, and D. R. Gamelin, *Nat. Mater.* **5**, 291 (2006).
- ⁴⁰C. A. Johnson, T. C. Kaspar, S. A. Chambers, G. M. Salley, and D. R. Gamelin, *Phys. Rev. B* **81**, 125206 (2010).
- ⁴¹M. Rohlfing and S. G. Louie, *Phys. Rev. B* **62**, 4927 (2000).